Available online at www.sciencedirect.com
ScienceDirect
Journal of Power Sources 179 (2008) 87–91
JOURNAL OF POWER SOURCES
www.elsevier.com/locate/jpowsour

Short communication

Catalytic behavior of Co_3O_4 in electroreduction of H_2O_2

Dianxue Cao *, Jundang Chao, Limei Sun, Guiling Wang

College of Material Science and Chemical Engineering, Harbin Engineering University, Harbin, 150001, PR China

Received 18 December 2007; accepted 19 December 2007
Available online 31 December 2007

Abstract

Spinel structure Co_3O_4 nanoparticles with an average diameter of around 17 nm were prepared and evaluated as electrocatalysts for H_2O_2 reduction. Results revealed that Co_3O_4 exhibits considerable activity and good stability for electrocatalytic reduction of H_2O_2 in 3 M NaOH solution. The reduction occurs mainly via the direct pathway when H_2O_2 concentration is lower than 0.5 M. An Al-H_2O_2 semi fuel cell using Co_3O_4 as cathode catalyst was constructed and tested at room temperature. The fuel cell displayed an open circuit voltage of 1.45 V and a peak power density of 190 mW cm^{-2} at a current density of 255 mA cm^{-2} operating with a catholyte containing 1.5 M H_2O_2. This study demonstrated that Co_3O_4 nanoparticles are promising cathode catalysts, in place of precious metals, for fuel cells using H_2O_2 as oxidant.

Keywords: Cobalt oxide; Hydrogen peroxide; Electrochemical reduction; Cathode catalyst; Metal semi fuel cell

1. Introduction

In recent years, hydrogen peroxide has been used as oxidant for several types of low temperature liquid-based fuel cells, including direct methanol-hydrogen peroxide fuel cell [1–3], direct borohydride-hydrogen peroxide fuel cell [4–10], hydrazine-hydrogen peroxide fuel cell [11], biofuel-hydrogen peroxide fuel cell [12–14], and metal-hydrogen peroxide semi fuel cell [15–22,2,23–25]. These fuel cells except biofuel cell have high energy density, high performance, compact design and workability in environments without air. Therefore, they are good candidates of underwater and space powers.

Comparing to oxygen, hydrogen peroxide has the following advantages when used as oxidant of fuel cells: (1) the electroreduction of hydrogen peroxide is a two-electron transfer process and hence has lower activation energy. The exchange current density of hydrogen peroxide reduction is around six order higher than that of oxygen reduction [26,27], so fuel cells using hydrogen peroxide as oxidant tend to provide higher performance than using oxygen; (2) hydrogen peroxide is in liquid form, its handling, storage and feeding to a fuel cell are easier than a gas phase oxidant, like oxygen. So fuel cell systems using hydrogen peroxide as cathode oxidant are more compact and convenient; (3) the electroreduction of liquid hydrogen peroxide on a fuel cell cathode occurs in a solid/liquid two-phase reaction zone, while oxygen electroreduction requires a solid/liquid/gas three-phase region (gas diffusion electrode). The two-phase reaction zone is readily realizable and much steady during fuel cell operation than the three-phase region.

Three types of electrocatalysts for hydrogen peroxide reduction have been investigated. They are: (1) noble metals, such as platinum, palladium, iridium, silver, gold, and a combination of these [4,7,10,17,19,21,22]; (2) macrocycle complexes of transition metals, such as Fe- and Co-porphyrin, Cu-triazine complexes [28–30]; (3) enzymes, such as peroxidase [13,31]. Nobel metal catalysts show high activity, however, they also catalyze the chemical decomposition of hydrogen peroxide to oxygen. The evolved oxygen, if not further reduced, will contribute little usable electrical energy, and therefore reduce the energy density of the system. Very recently, Gu et al. identified gold to be an effective catalyst using Pourbaix diagrams to guide experimental testing. They found that Au/C minimizes gas evolution of hydrogen peroxide while providing relatively high power density [10]. Enzymes are remarkable as hydrogen peroxide electroreduction catalysts showing high reduction potential and no excessive oxygen evolution [31]. However, they generally require specific environments, are not robust enough to handle high concentration hydrogen peroxide or temperature

* Corresponding author. Tel.: +86 451 82589036; fax: +86 451 82589036.
E-mail address: caodianxue@hrbeu.edu.cn (D. Cao).

0378-7753/$ – see front matter © 2007 Elsevier B.V. All rights reserved.
doi:10.1016/j.jpowsour.2007.12.076

ranges, and do not have the lifetime of conventional noble metal catalysts. Macrocycle complexes of transition metals are less active than noble metal catalysts. Their stability in high concentration hydrogen peroxide needs to be improved.

Cobalt oxides have captured considerable attention due to their low cost, wide availability, stability in alkaline solution and good electrocatalytic properties as oxygen evolution and reduction catalysts [32]. In this paper, the electrocatalytic activity and stability of Co_3O_4 for hydrogen peroxide reduction were investigated. The performance of Co_3O_4 as the cathode catalyst of an alkaline aluminum-hydrogen peroxide semi fuel cell was evaluated.

2. Experimental

Co_3O_4 powders were synthesized by a precipitation method. $Co(NO_3)_2{\cdot}6H_2O$ (>99.0%) and NH_4HCO_3 (NH_4 21.0–22.0%) were used as source materials. An aqueous solution of NH_4HCO_3 was added dropwise to an aqueous solution of $Co(NO_3)_2$ at room temperature under constant stirring condition. The mole ratio of $Co(NO_3)_2$ to NH_4HCO_3 was 1:2.2. The obtained precipitates were separated from the solution by vacuum filtration, washed with distilled water, and dried at 100 °C in an oven for 1 h. The resulting solid products were then grounded to fine powders and calcined at 350 °C for 3 h. The phase and average particle size of the final products were determined using an X-ray diffractometer (XRD, Rigaku TTR III) with Cu Kα radiation (λ = 1.51406 nm). The 2θ scan range is from 10° to 80° with a scan rate of 5° min^{-1} and a step width of 0.01°.

Co_3O_4 electrodes were prepared as follows: Co_3O_4 nanoparticles and carbon black (Vulcan XC-72) were dispersed in anhydrous ethanol and sonicated for 10 min to obtain a suspension, to which, a PTFE emulsion was added. The mixture was sonicated for 15 min and then heated at 80 °C in a water bath until a thick paste was formed. The paste was filled in pores of nickel foam using a doctor blade. The nickel foam containing the paste was then heated at 80 °C until completely dry. The evaporation of solvents results in the formation of micro-channels within the electrode. These channels provided pathways for the transfer of electrolyte, reactants and products. The nickel foam served as both the current collector and the matrix for retaining electrode materials. The dry weight ratio of Co_3O_4 to carbon black is 7:3 and the ratio of carbon black to PTFE is 3:1. Prior to use, nickel foams were degreased with acetone, etched with 6.0 M HCl for 15 min, rinsed with ultrapure water and used immediately.

Electrochemical measurements were carried out in a standard three-electrode electrochemical cell with saturated Ag/AgCl reference electrode and glassy carbon rod (behind a D-porosity glass frit) counter electrode. The Co_3O_4 working electrode has a dimension of 10 mm × 10 mm × 0.5 mm and a Co_3O_4 loading of around 15 mg cm^{-2}. The reported currents were normalized by the geometrical area of Co_3O_4 electrodes. Cyclic voltammetry and chronoamperometry were conducted using a computerized VMP3/Z potentiostat (Princeton Applied Research) controlled by the EC-lab software.

The performance of Co_3O_4 electrode as cathode of an Al-H_2O_2 semi fuel cell was examined using a home-made flow through test cell made of Plexiglas. The electrode area was 4.0 cm^2 (20 mm × 20 mm). Aluminum alloy LF6 (91.9%Al, 6.5%Mg, 0.6%Mn, 0.3%Fe, 0.3%Si, 0.2%Zn, 0.1Ti%) served as anode. Nafion-115 (DuPont) was used as membrane to separate the anode and the cathode compartments. The anolyte (3.0 M NaOH) and the catholyte (3.0 M NaOH + H_2O_2) were pumped into the bottom of the anode and the cathode compartments, respectively, and exited at the top of the compartments. The flow rate is 100 mL min^{-1} for both the anolyte and the catholyte and is controlled by individual peristaltic pump. The cell voltage–current curves were recorded using a computer-controlled E-load system (Arbin).

All measurements were performed at room temperature using 3.0 M NaOH as electrolytes. All solutions were made with analytical grade chemical reagents and Milli-Q water (Millipore, 18 MΩ cm). All potentials were reported versus Ag/AgCl (sat. KCl) electrode.

3. Results and discussion

Fig. 1 shows the X-ray diffraction pattern of the synthesized sample and the standard crystallographic spectrum of spinel Co_3O_4 from JCPDS card 00-042-1467 (vertical lines). It can be seen that the pattern of our synthesized sample matches well with the standard crystallographic pattern of Co_3O_4, and only peaks due to the reflections of Co_3O_4 are visible. These results indicated that the synthesized sample is pure Co_3O_4 with spinel structure [33,34]. The average crystallite size was about 17 nm estimated using the Scherrer's equation.

The catalytic activity of Co_3O_4 for H_2O_2 electroreduction was studied using cyclic voltammetry and the results are presented in Fig. 2. Curve (a) shows the cyclic voltammogram (CV) of Co_3O_4 recorded in 3.0 M NaOH containing 0.6 M H_2O_2 at a scan rate of 5mV s^{-1}. As can be seen that the onset potential for H_2O_2 reduction is around −0.15 V. A limiting current density of around 110 mA cm^{-2} was achieved at around −0.4 V. The current increases linearly with the decrease of potential in the negative going scan. In order to clarify that the cathodic currents were not from the reduction of Co_3O_4 electrode, a CV of Co_3O_4 electrode was measured in 3.0 M NaOH containing no H_2O_2 (insert, curve (b)). A clear redox couple was observed with

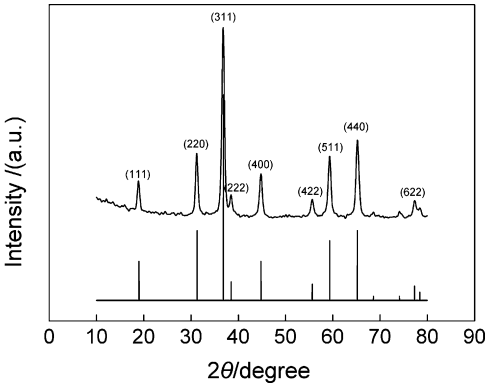

Fig. 1. XRD pattern of Co_3O_4. The vertical lines are from the standard crystallographic tables JCPDS card 00-042-1467.

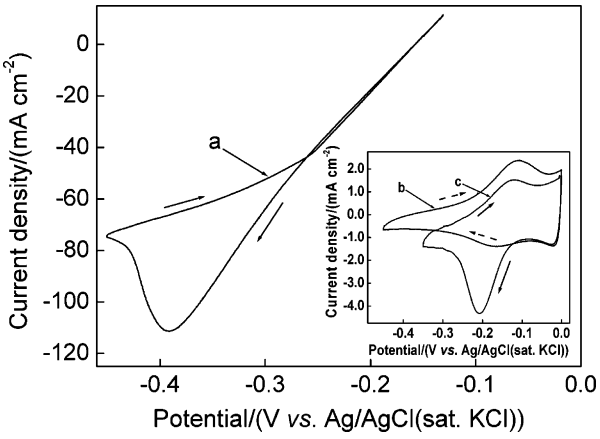

Fig. 2. Cyclic voltammograms of Co_3O_4 recorded in 3.0 M NaOH + 0.6 M H_2O_2 (a), 3.0 M NaOH (b) and O_2-saturated 3.0 M NaOH (c). The scan rate is 5 mV s^{-1}.

the anodic peak at −0.1 V and the cathodic peak at −0.16 V. This couple can be attributed to the conversion between $Co(OH)_2$ and Co_3O_4 ($3Co(OH)_2 + 2OH^- = Co_3O_4 + 4H_2O + 2e^-$) according to literatures [35,36]. The comparison of curve (a) and curve (b) clearly shows that cathodic currents generated by the electroreduction of Co_3O_4 were significantly lower than the currents from the H_2O_2 electroreduction. This result confirmed that Co_3O_4 demonstrated considerable catalytic activity for H_2O_2 electroreduction.

It is well known that the electroreduction of H_2O_2 can proceed through direct and indirect pathways. The direct reduction occurs via a two-electron process ($H_2O_2 + 2e^- \rightarrow 2OH^-$). The indirect reduction consists of the decomposition of H_2O_2 to O_2 followed by electroreduction of the latter. The direct reduction is the preferred pathway. We indeed observed the chemical decomposition of hydrogen peroxide on Co_3O_4 electrodes, particularly at concentrations of H_2O_2 higher than 0.6 M. It has been reported that Co_3O_4 exhibits activity for O_2 electroreduction in alkaline medium [37]. Therefore, the electroreduction of H_2O_2 on Co_3O_4 nanoparticles might proceed through the direct or the indirect pathway or both. In order to investigate via which pathway H_2O_2 reduction on Co_3O_4 occurs, the CV of Co_3O_4 electrode was measured in 3.0 M NaOH solution saturated with oxygen (insert, curve (c)). An oxygen reduction peak was observed. The peak has an onset potential of −0.1 V and a peak current density of 4.3 mA cm^{-2}. Clearly, the current density from the reduction of O_2 is much lower than that from H_2O_2 reduction. For example, at −0.2 V, the current generated by O_2 reduction is nearly five times lower than that from H_2O_2 reduction. So it can be concluded that hydrogen peroxide reduction on Co_3O_4 mainly proceeds through the direct pathway. The onset potentials for H_2O_2 and O_2 reductions are close to the cathodic peak potential of the $Co(OH)_2/Co_3O_4$ redox couple (around −0.15 V). This suggests that the $Co(OH)_2/Co_3O_4$ surface redox couple might be responsible for the activity of Co_3O_4.

The effects of hydrogen peroxide concentration on the catalytic behavior of Co_3O_4 were investigated and the results are given in Fig. 3. It was found that cathodic peak currents increased approximately linearly with the increase of H_2O_2 concentration from 0.2 to 2.0 M, demonstrating that the reduction reaction at the peak potential is diffusion-controlled. When the hydrogen peroxide concentration increased from 0.6 to 0.8 M, the onset potential shifted to negative side by around 40 mV. This shift might result from the decomposition of H_2O_2, which was observed (indicated by the formation of small bubbles on electrode surface) at hydrogen peroxide concentration higher than 0.8 M. A current density of as high as 260 mA cm^{-2} was achieved at 1.5 M hydrogen peroxide, of course at the expense of significant H_2O_2 decomposition.

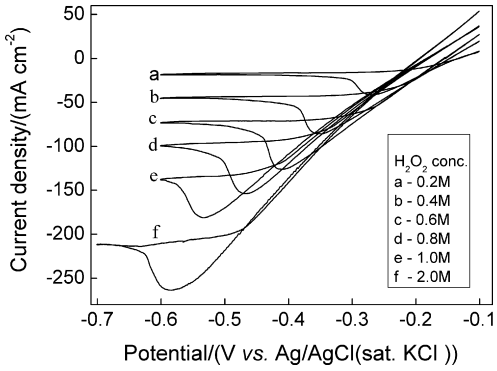

Fig. 3. Cyclic voltammograms of Co_3O_4 measured in 3.0 M NaOH containing H_2O_2 with different concentrations between 0.2 and 2.0 M. The scan rate is 5 mV s^{-1}.

Fig. 4 demonstrates chronoamperometric curves for hydrogen peroxide reduction measured in 3.0 M NaOH containing 0.6 M H_2O_2. At the mixed kinetic-diffusion control potentials (−0.2 and −0.3 V), currents reached to steady-state after a few seconds and displayed no decrease within 30 min test period, indicating Co_3O_4 have a good stability for hydrogen peroxide reduction. At the diffusion-control potential (−0.4 V), currents fluctuated and decreased slightly with the increase of time. This behavior likely results from the depletion of H_2O_2 near the electrode surface.

An aluminum-hydrogen peroxide single semi fuel cell was constructed in order to evaluate the performance of Co_3O_4 as cathode catalysts. The anode is a 20 mm × 20 mm × 0.7 mm aluminum alloy LF6. The cathode is a 20 mm × 20 mm × 0.5 mm Co_3O_4 electrode with Co_3O_4 loading of 15 mg cm^{-2}. A Nafion-115 membrane was sandwiched between the anode and the

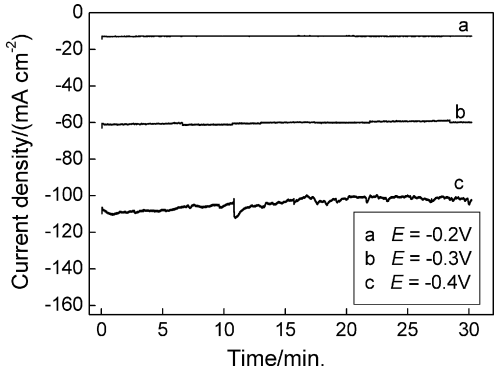

Fig. 4. Chronoamperometric curves for H_2O_2 reduction at different potentials in 3.0 M NaOH + 0.6 M H_2O_2.

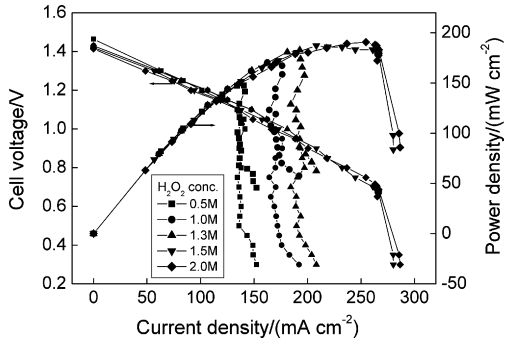

Fig. 5. Performance of Al-H_2O_2 single semi fuel cell with Co_3O_4 cathode operating at room temperature. The catholytes are 3.0 M NaOH containing H_2O_2 with different concentrations.

cathode. Fig. 5 shows the cell voltage and power density versus current density curves recorded with varying concentrations of H_2O_2 feeding to the cathode compartment. An open circuit voltage of around 1.45 V was obtained. The cell voltage decays linearly with the increase of current density until reaching to the mass transport control region, and then drops rapidly. This observation indicated that the cell performance shows a strong dependence on the ohmic resistance of the cell. Overvoltages due to kinetic limitations cannot be seen as they are probably masked by IR drop. The increase of H_2O_2 concentration did not significantly affect the linear portion of the polarization curves, but led to a significant increase in mass transport limiting currents. For example, the limiting current density increased from 140 mA cm^{-2} at 1.05 V to 265 mA cm^{-2} at 0.67 V when the concentration of H_2O_2 increased from 0.5 to 2.0 M. Decomposition of H_2O_2 occurred at concentration higher than 1.0 M, however, it did not cause significant cell performance drop. The power density–current density curves exhibited maximum power densities of 147 mW cm^{-2} at 140 mA cm^{-2} operating on 0.5 M H_2O_2 and 190 mW cm^{-2} at 255 mA cm^{-2} running on 1.5 M H_2O_2.

It should be pointed out that the Al-H_2O_2 semi fuel cell presented in this work is only for demonstrating the feasibility of Co_3O_4 as cathode catalysts of a fuel cell. The cell configuration, cathode structure and operation conditions (i.e. temperature, flow rate) were not optimized. The cell performance can be enhanced, for example, by reducing IR drop and by modifying the Co_3O_4 cathode structure to improve the mass transport of H_2O_2 within the electrode. It is worth to emphasize that, except serving as cathode catalysts of Al-H_2O_2 semi fuel cells, Co_3O_4 can also be used as cathode catalysts for other types of fuel cells using H_2O_2 as oxidant, e.g. direct $NaBH_4$-H_2O_2 fuel cells. When acting as the cathode catalyst of a direct $NaBH_4$-H_2O_2 fuel cell, Co_3O_4 may have great advantages over precious metal catalysts because it is probably borohydride tolerant [38]. The problem of Co_3O_4 as H_2O_2 reduction electrocatalysts is the oxygen evolution from chemical decomposition of H_2O_2, which, however, can be minimized by structure modification [34]. The performance of Co_3O_4 as cathode catalysts for direct $NaBH_4$-H_2O_2 fuel cells (e.g. tolerance to borohydride) and measures for reducing oxygen evolution are under investigation in our laboratory.

4. Conclusions

Nano-sized spinel Co_3O_4 powders were synthesized and their performances as H_2O_2 electroreduction catalysts were investigated. It was found that Co_3O_4 nanoparticles displayed considerable activity and good stability for H_2O_2 electroreduction in alkaline electrolyte. The chemical decomposition of H_2O_2 on Co_3O_4 is insignificant at H_2O_2 concentration lower than 0.5 M, and it has no remarkable negative effects on the electroreduction of H_2O_2 via the direct pathway. An Al-H_2O_2 semi fuel cell using Co_3O_4 as the cathode catalyst displayed an open circuit voltage of 1.45 V and peak power densities of 147 mW cm^{-2} at 140 mA cm^{-2} operating on 0.5 M H_2O_2 and 190 mW cm^{-2} at 255 mA cm^{-2} running on 1.5 M H_2O_2. This study shows that Co_3O_4 nanoparticles are promising cathode catalysts for fuel cells using H_2O_2 as oxidant.

Acknowledgement

This work was financially supported by Harbin Engineering University through the foundation for the innovation platform of underwater power source (HEUFT07030).

References

[1] W. Sung, J.W. Choi, J. Power Sources 172 (2007) 198.
[2] T. Bewer, T. Beckmann, H. Dohle, J. Mergel, D. Stolten, J. Power Sources 125 (2004) 1.
[3] D.N. Prater, J.J. Rusek, Appl. Energy 74 (2003) 135.
[4] G.H. Miley, N. Luo, J. Mather, R. Burton, G. Hawkins, L. Gu, E. Byrd, R. Gimlin, P.J. Shrestha, G. Benavides, J. Laystrom, D. Carroll, J. Power Sources 165 (2007) 509.
[5] C.P. de Leon, F.C. Walsh, A. Rose, J.B. Lakeman, D.J. Browning, R.W. Reeve, J. Power Sources 164 (2007) 441.
[6] R.K. Raman, A.K. Shukla, Fuel Cells 7 (2007) 225.
[7] R.K. Raman, N.A. Choudhury, A.K. Shukla, Electrochem. Solid-State Lett. 7 (2004) 488.
[8] R.K. Raman, S.K. Prashant, A.K. Shukla, J. Power Sources 162 (2006) 1073.
[9] N.A. Choudhury, R.K. Raman, S. Sampath, A.K. Shukla, J. Power Sources 143 (2005) 1.
[10] L. Gu, N. Luo, G.H. Miley, J. Power Sources 173 (2007) 77.
[11] H.B. Urbach, R.J. Bowen, J. Electrochem. Soc. 117 (1970) 1594.
[12] B. Tartakovsky, S.R. Guiot, Biotechnol. Prog. 22 (2006) 241.
[13] A. Pizzariello, M. Stred'ansky, S. Miertus, Bioelectrochemistry 56 (2002) 99.
[14] A. Ramanavicius, A. Kausaite, A. Ramanaviciene, Biosensors Bioelectron. 20 (2005) 1962.
[15] O. Hasvold, K.H. Johansen, O. Mollestad, S. Forseth, N. Storkersen, J. Power Sources 80 (1999) 254.
[16] D.J. Brodrecht, J.J. Rusek, Appl. Energy 74 (2003) 113.
[17] R.R. Bessette, M.G. Medeiros, C.J. Patrissi, C.M. Deschenes, C.N. LaFratta, J. Power Sources 96 (2001) 240.
[18] E.G. Dow, R.R. Bessette, G.L. Seeback, C. Marsh-Orndorff, H. Meunier, J. VanZee, M.G. Medeiros, J. Power Sources 65 (1997) 207.
[19] M.G. Medeiros, E.G. Dow, J. Power Sources 80 (1999) 78.
[20] M.G. Medeiros, R.R. Bessette, C.M. Deschenes, C.J. Patrissi, L.G. Carreiro, S.P. Tucker, D.W. Atwater, J. Power Sources 136 (2004) 226.
[21] W. Yang, S. Yang, W. Sun, G. Sun, Q. Xin, Electrochim. Acta 52 (2006) 9.
[22] W. Yang, S. Yang, W. Sun, G. Sun, Q. Xin, J. Power Sources 160 (2006) 1420.
[23] M.G. Medeiros, R.R. Bessette, C.M. Deschenes, D.W. Atwater, J. Power Sources 96 (2001) 236.

[24] R.R. Bessette, J.M. Cichon, D.W. Dischert, E.G. Dow, J. Power Sources 80 (1999) 248.
[25] O. Hasvold, N.J. Storkersen, S. Forseth, T. Lian, J. Power Sources 162 (2006) 935.
[26] R. O'Hayre, S.W. Cha, W. Colella, F.B. Prinz, Fuel Cell Fundamentals, Wiley, New York, 2006.
[27] N. Luo, G.H. Miley, P.J. Shrestha, R. Gimlin, R. Burton, G. Hawkins, J. Mather, J. Rusek, F. Holcomb, in: Proceeding of Eighth International Hydrogen Peroxide Propulsion Conference, Purdue University, Lafayette,IN, USA, 2005, p. 87–96.
[28] H. Liu, L. Zhang, J. Zhang, D. Ghosh, J. Jung, B.W. Downing, E. Whittemore, J. Power Sources 161 (2006) 743.
[29] R.K. Raman, A.K. Shukla, J. Appl. Electrochem. 35 (2005) 1157.
[30] V.L.N. Dias, E.N. Fernandes, L.M.S. da Silva, E.P. Marques, J. Zhang, A.L.B. Marques, J. Power Sources 142 (2005) 10.
[31] D.N. Prater, J.J. Rusek, in: Proceedings of the Sixth European Space Power Conference (ESPC), ESA/ESTEC, Porto, Portugal, 2002, p. 705.
[32] S. Palmas, F. Ferrara, A. Vacca, M. Mascia, A.M. Polcaro, Electrochim. Acta 53 (2007) 400.
[33] V.A. de la Pena O'Shea, N. Homs, E.B. Pereira, R. Nafria, P. Ramirez de la Piscina, Catal. Today 126 (2007) 148.
[34] N.A.M. Deraz, Mater. Lett. 57 (2002) 914.
[35] I.G. Casella, M. Gatta, J. Electroanal. Chem. 534 (2002) 31.
[36] C. Barbero, G.A. Planes, M.C. Miras, Electrochem. Commun. 3 (2001) 113.
[37] R.N. Singh, J.F. Koenig, G. Poillerat, P. Chartier, J. Electroanal. Chem. 314 (1991) 241.
[38] R.X. Feng, H. Dong, Y.D. Wang, X.P. Ai, Y.L. Cao, H.X. Yang, Electrochem. Commun. 7 (2005) 449.